# Learning to Equalize: Data-Driven Frequency-Domain Signal Recovery in Molecular Communications

Cheng Xiang, Yu Huang, *Member, IEEE,* Miaowen Wen, *Senior Member, IEEE,* Weiqiang Tan, and Chan-Byoung Chae, *Fellow, IEEE*



***Abstract*—In molecular communications (MC), inter-symbol interference (ISI) and noise are key factors that degrade communication reliability. Although time-domain equalization can effectively mitigate these effects, it often entails high computational complexity concerning the channel memory. In contrast, frequency-domain equalization (FDE) offers greater computational efficiency but typically requires prior knowledge of the channel model. To address this limitation, this letter proposes FDE techniques based on long short-term memory (LSTM) neural networks, enabling temporal correlation modeling in MC channels to improve ISI and noise suppression. To eliminate the reliance on prior channel information in conventional FDE methods, a supervised training strategy is employed for channel-adaptive equalization. Simulation results demonstrate that the proposed LSTM-FDE significantly reduces the bit error rate compared to traditional FDE and feedforward neural network–based equalizers. This performance gain is attributed to the LSTM's temporal modeling capabilities, which enhance noise suppression and accelerate model convergence, while maintaining comparable computational efficiency.**

***Index Terms*—Diffusion channel, frequency domain equalization, machine learning, molecular communication, signal detection.**

## I. Introduction

MOLECULAR communication (MC) is an emerging paradigm that enables information transmission at the nanoscale. Unlike traditional wireless systems that rely on electromagnetic waves, MC employs chemical or biological molecules as carriers, offering high biocompatibility and excellent energy efficiency [1], [2]. These characteristics make MC highly promising for applications in biomedical engineering, such as targeted drug delivery and in-body monitoring [3].

Practical deployment of MC, however, faces significant challenges. Noise processes in MC differ fundamentally from those in electromagnetic communication. Molecular noise includes both signal-independent and signal-dependent components, the latter arising from fluctuations in molecule concentration and stochastic receptor binding [4]. In addition, signal propagation depends on diffusion and other physical mechanisms (e.g., fluid flow, chemical reactions) [5], making channels highly sensitive to environmental variations and prone to random delays [6]. Moreover, temporal overlap between consecutive symbols induces severe inter-symbol interference (ISI), which degrades detection accuracy. To mitigate ISI, time-domain equalization (TDE) methods such as MMSE and decision feedback equalizers have been thoroughly studied in MC. While MMSE equalizers reduce symbol errors, their quadratic complexity with respect to ISI length limits real-time applicability [7]. Decision feedback equalizers can further suppress residual interference but suffer from error propagation in low-SNR regimes [8]. Alternative strategies, including controlled molecule release and MIMO techniques, have also been explored [9]. Nevertheless, these approaches remain constrained by computational overhead and the requirement of accurate channel estimation.

Frequency-domain equalization (FDE) provides an efficient alternative to TDE for ISI mitigation [10]. Unlike TDE, whose complexity scales with ISI length, FDE leverages frequency-domain processing to reduce computational load while achieving comparable performance, particularly at high data rates. However, like TDE, FDE critically depends on accurate channel state information (CSI). The time-varying nature of MC channels, stochastic perturbations from Brownian motion, and complex noise statistics complicate precise channel estimation, thereby limiting the effectiveness of model-based equalizers.

Data-driven machine learning (ML) approaches have recently emerged as a promising solution. By training on large datasets, ML methods can inherently capture nonlinear and time-varying channel characteristics without explicit analytical modeling. Furthermore, they adapt to variations in noise statistics, improving robustness and ensuring reliable detection across diverse channel conditions. Yet, existing ML-based equalizers in MC have almost exclusively focused on time-domain representations.

In contrast to prior MC studies where ML has been exclusively applied in the time domain, we propose an LSTM-FDE framework that reformulates signal recovery in the frequency domain. This design is inspired by the advance in computer vision [11], which demonstrated that frequency-domain features can serve as effective inputs for neural networks and even outperform conventional spatial-domain learning with

X. Cheng and Y. Huang are with the Research Center of Intelligent Communication Engineering, School of Electronics and Communication Engineering, Guangzhou University, Guangzhou 510006, China (e-mail: 2112330087@e.gzhu.edu.cn; yuhuang@gzhu.edu.cn).

M. Wen is with Guangdong Provincial Key Laboratory of Short-Range Wireless Detection and Communication, School of Electronic and Information Engineering, South China University of Technology, Guangzhou 510641, China (e-mail: eemwwen@scut.edu.cn).

W. Tan is with the School of Computer Science and Cyber Engineering, Guangzhou University, Guangzhou 510006, China (e-mail: wqtan@gzhu.edu.cn).

C.-B. Chae is with the School of Integrated Technology, Yonsei University, Seoul 03722, South Korea (e-mail: cbchae@yonsei.ac.kr).

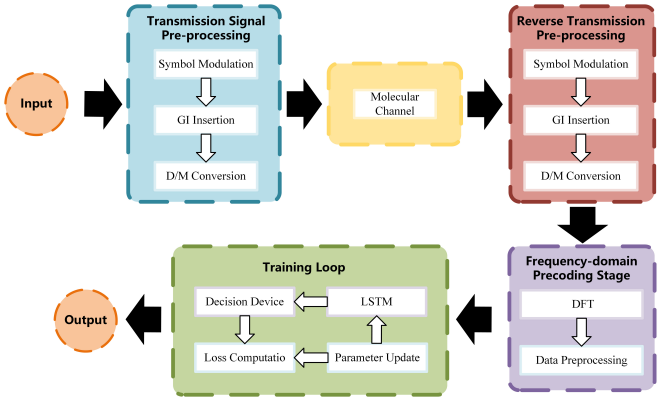


Fig. 1. Structure diagram of LSTM-FDE.

minimal structural changes. Enlightened by its success and the effectiveness of the FDE paradigm for low-complexity MC signal detection [10], we present, to the best of our knowledge, the first frequency-domain learning framework for MC as illustrated in Fig. 1, where the conventional detector is replaced with an LSTM-based network, which models temporal dependencies in molecular signals while reducing the overall computational complexity. Overall, the main contributions of this letter can be summarized as follows:

- We introduce a data-driven frequency-domain framework for signal recovery in MC, extending ML-based detection beyond conventional time-domain approaches.
- A low-complexity LSTM-FDE detector is proposed for MC systems, which reduces computational complexity relative to its time-domain counterparts.
- We provide a comprehensive evaluation of error performance by benchmarking LSTM-FDE against FNN-FDE and GRU-FDE under various transmission rate scenarios and noise conditions, demonstrating its improved robustness and generalization.

The remainder of this letter is organized as follows. Section II describes the system model. Section III introduces the proposed LSTM-FDE and comparative methods. Section IV presents simulation results and performance analysis. Finally, Section V concludes the letter.

## II. System Model

This letter employs a classical single-input single-output MC model. The core components consist of a point-source transmitter, a free-diffusion channel, and a passive spherical receiver with radius $r$. The transmitter releases molecules through on-off keying (OOK), with the propagation of information molecules governed by Fick's laws of diffusion in the channel. The receiver passively counts molecules arriving within its surface boundary without absorption or consumption. For the OOK scheme, the transmitted signal at time $t$ is defined as

$$q(t) = \begin{cases} Q, & \text{bit-1}, \\ 0, & \text{bit-0}, \end{cases} \tag{1}$$

where $Q$ denotes the number of molecules released by the transmitter when sending bit "1", with no molecules emitted for bit "0". The channel impulse response (CIR) of this model has been rigorously derived in [5]. Assume that molecules are released from the origin and undergo random diffusion through Brownian motion in a free diffusion channel. The receiver is a sphere with radius $r$. When the distance $d$ between the receiver and the transmitter remains constant, the channel environment is stable, and the condition $d \gg r$ holds, the CIR of this model in an infinite three-dimensional space can be expressed based on Fick's second law as [12]

$$h(t) = \frac{V_{\mathrm{r}}}{(4\pi D t)^{\frac{3}{2}}} \exp\left(-\frac{d^2}{4Dt}\right) \tag{2}$$

where $d$ is the distance between the transmitter and the receiver, $D$ represents the diffusion coefficient, $t$ denotes time, and $V_{\mathrm{r}} = \frac{4}{3}\pi r^3$ is the volume of the receiver. To model ISI, appropriate delays are introduced during symbol transmission:

$$r(t) = \sum_{\ell=0}^{L} h(t - \ell T_{\mathrm{sym}}) \cdot q(t - \ell T_{\mathrm{sym}}), \tag{3}$$

where $L$ indicates the ISI length and $T_{\mathrm{sym}}$ denotes the symbol duration.

In our model, two types of noise are considered: signal-dependent noise $n_s(t)$ and signal-independent noise $n_i(t)$. The signal-dependent noise originates from the inherent randomness of diffusion, which induces fluctuations in the received signal. This component is modeled as a zero-mean Gaussian random variable with signal-dependent variance, i.e.,$n_s(t) \sim \mathcal{N}\left(0, \frac{r(t)}{V_r}\right)$. The signal-independent noise, in contrast, reflects the background effect and is modeled as a zero-mean Gaussian random variable with constant variance, i.e., $n_i(t) \sim \mathcal{N}(0, \sigma^2)$. Accordingly, the received signal is expressed as

$$y(t) = r(t) + n_s(t) + n_i(t). \tag{4}$$

The Gaussian model is widely employed in noise modeling for MC, owing to its physical relevance in diffusion-based channels as well as its analytical tractability [13]. Training data for the LSTM-FDE equalizer are generated under this assumption. Nonetheless, its data-driven structure enables robustness against deviations from Gaussian statistics in real environments.

## III. Data-Driven Methods for Frequency Domain Equalization

This section introduces three data-driven FDE methods. We first analyze the time complexity of these three methods, and then compare them with other common approaches to assess their performance and applicability.

### A. Data-Driven Methods

*1) FNN Architecture:* A Feedforward neural network (FNN) is a commonly used neural network architecture where each neuron is connected to all neurons in the previous layer. It captures the nonlinear relationships of input signals through a multilayer perceptron (MLP) and learns the mapping between input and target signals for signal recovery. Compared

TABLE I
TIME COMPLEXITY OF DIFFERENT ALGORITHMS

| Algorithm | Time Complexity |
|---|---|
| ZF-FDE [10] | $\mathcal{O}(M \log_2 M)$ |
| Statistical MMSE-FDE [10] | $\mathcal{O}(M \log_2 M)$ |
| $i$-times Iterative MMSE-FDE [10] | $\mathcal{O}(iM \log_2 M)$ |
| FNN-FDE | $\mathcal{O}(LM\nu)$ |
| LSTM-TDE | $\mathcal{O}\big(L(S+1)\nu + 4L\nu^2\big)$ |
| LSTM-FDE | $\mathcal{O}\left(L \log M + L\nu + \frac{4L\nu^2}{M}\right)$ |
| GRU-FDE | $\mathcal{O}\left(L \log M + L\nu + \frac{3L\nu^2}{M}\right)$ |

to recurrent neural network (RNN), FNNs lack a memory mechanism and struggle with long-term dependencies, but due to its lower computational complexity, it is efficient for short-term dependencies.

*2) GRU Architecture:* The gated recurrent unit (GRU) is a streamlined RNN that merges LSTM's forget and input gates into a single update gate and replaces the cell state with a hidden state, reducing parameters and training effort. In FDE for MC, the update gate balances residual molecular effects with the current symbol's response, while the reset gate controls past-state influence in new activations. This compact architecture captures long-term dependencies at lower cost than LSTMs, offering an efficient trade-off between ISI suppression and complexity.

*3) LSTM Architecture:* LSTM, a variant of RNNs, uses gating mechanisms to capture long-term dependencies while mitigating gradient issues. In FDE for MC, its gates have clear physical meanings: the forget gate models the diffusion-dependent decay of residual molecules, the input gate scales the current symbol's impulse response, and the cell state integrates molecule counts over time. This structure adaptively re-weights frequency components, improving signal quality in noisy conditions and outperforming feedforward networks in ISI suppression, despite higher training costs.

### B. Data Processing

Based on the simulation dataset generated from the system model described in Section II, we first convert the dataset from the time domain to the frequency domain

$$Y(m) = \sum_{t=0}^{M-1} y(t) \cdot e^{-j2\pi mt/M}, \quad m = 0, 1, \ldots, M-1 \quad (5)$$

where $M$ represents the number of frequency-domain bins, and the frequency-domain coefficients of each symbol block are arranged in ascending order of frequency, where low-frequency components correspond to slow diffusion processes, while high-frequency components correspond to fast diffusion dynamics. To eliminate the dimensional disparity in amplitude and accelerate model convergence, we apply min-max normalisation to map the values to the [0, 1] range. To avoid numerical instability, a small constant $\epsilon$ is introduced in the denominator

$$\tilde{Y}[m] = \frac{|Y[m]| - \text{Min}}{\text{Max} - \text{Min} + \epsilon}, \quad (6)$$

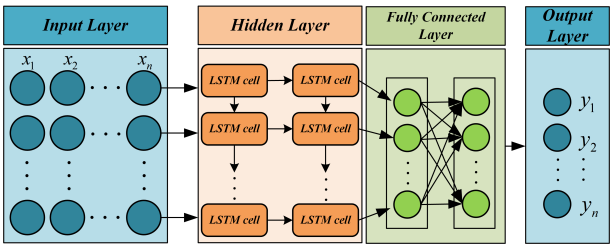


Fig. 2. Block diagram of the LSTM-FDE training process.

where Max and Min denote the maximum and minimum values of the frequency-domain magnitude within the current symbol, respectively. The normalized sequence is fed into the LSTM in chronological order for training. This architecture characterizes the diffusion time scale through the frequency sequence, thereby enabling joint time–frequency modeling. The processed sequence is then passed through the LSTM network, whose output is subsequently mapped to an equalized signal by a fully connected layer. The output of the fully-connected layer is the equalized signal $o[m]$. This signal is then demodulated by a decision module to recover the original bit sequence. Given the use of OOK modulation and the Sigmoid activation function in the output layer of the LSTM, a fixed threshold of 0.5 is applied: if $o[m] \geq 0.5$, the bit is decoded as "1"; otherwise, it is decoded as "0".

### C. Complexity Comparison

Table I summarizes the time complexity of various equalization algorithms. Key parameters are defined as follows: $L$ is the total number of transmitted symbols, $v$ is the number of hidden units in the LSTM or GRU network, $i$ is the number of iterations in iterative MMSE-FDE, and $S$ denotes the length of ISI in the time domain.

The key difference between time-domain and frequency-domain methods lies in how they handle ISI. Time-domain approaches, such as TDE-LSTM, explicitly process ISI using a window of size $S+1$, resulting in a $\mathcal{O}(LSv)$ complexity that grows linearly with the ISI length. In contrast, the proposed LSTM-FDE and GRU-FDE operate in the frequency domain, parallelizing ISI mitigation and eliminating dependence on $S$, which greatly reduces computation. Similarly, FNN-FDE uses a fully connected architecture with a low computational complexity of $\mathcal{O}(LMv)$.

Frequency-domain methods offer significant complexity advantages. Model-based techniques such as ZF-FDE and MMSE-FDE achieve $\mathcal{O}(M \log_2 M)$ complexity using FFT operations, while iterative MMSE-FDE requires $\mathcal{O}(iM \log_2 M)$ due to multiple iterations. The proposed LSTM-FDE and GRU-FDE further improve efficiency with $\mathcal{O}(L \log M)$ complexity, providing substantial savings in long-ISI scenarios. Among data-driven approaches, FNN-FDE has the lowest complexity but suffers in challenging ISI conditions due to the lack of temporal memory. Moreover, these methods avoid explicit channel estimation, reducing overhead and enhancing robustness in dynamic channels.

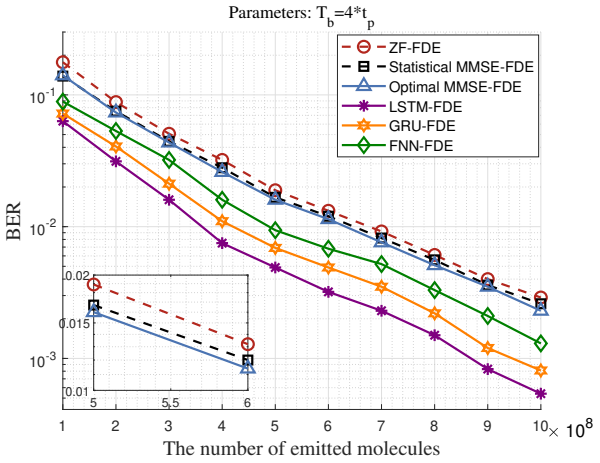


Fig. 3. The BER performance of various FDEs at $T_b = 4 * t_p$, showing LSTM-FDE's clear advantage over traditional methods.

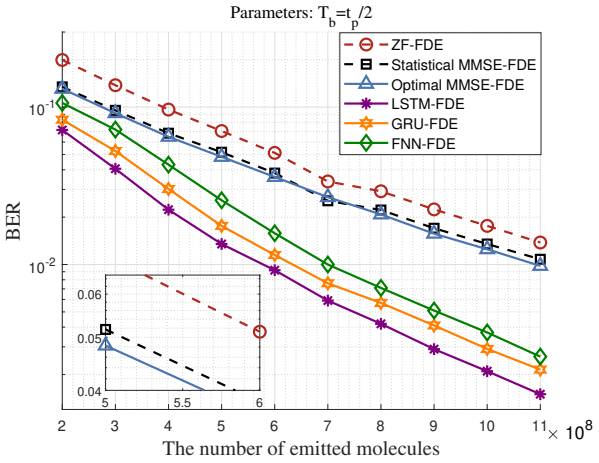


Fig. 4. The BER performance of various FDEs when the symbol duration $T_b = t_p/2$.

TABLE II
COMPARISON OF MODEL HYPERPARAMETER CONFIGURATIONS

| Parameter | LSTM Model | GRU Model | FNN Model |
|---|---|---|---|
| Optimizer | Adam | Adam | Adam |
| Learning Rate | 0.001 | 0.001 | 0.002 |
| Training Epochs | 30 | 30 | 120 |
| Hidden Units/Layer Structure | 60 | 60 | [256, 128] |
| Activation Function | Tanh | Tanh | ReLU |
| Recurrent Layers | 2 | 2 | – |
| Batch Size | 64 | 64 | 128 |

## IV. Simulation Setup and Results Analysis

In this section, we present a detailed description of the parameter settings for the simulation experiments and evaluate and compare the performance of each equalization method.

### A. Simulation Setup

To characterize the simulated MC system, we define the parameter $t_p = \frac{d^2}{6D}$, which denotes the time at which the molecular concentration peaks at the receiver. A dataset consisting of 4,000,000 randomly generated binary symbols ("0" or "1") was created, and we followed the steps outlined in Section III to complete the data preprocessing. The dataset was then split into training, validation, and test sets in a 60%, 20%, and 20% ratio. This preprocessed dataset is utilized to train an LSTM-based detection system in a supervised manner. Within this system, a FDE is embedded and adaptively optimized. The learnable parameters subject to optimization include the equalizer coefficients, collectively denoted as

$$W = \{W_f, W_i, W_c\}, \tag{7}$$

where $W_f$, $W_i$, and $W_c$ represent the weight matrices corresponding to the forget gate, input gate, and cell state of the LSTM, respectively. This optimization is performed without explicit CSI. The binary cross-entropy (BCE) loss function is adopted to quantify the detection accuracy by measuring the discrepancy between the equalizer's output probability $p_\ell$ and the true transmitted bit $b_\ell$. The loss function is defined as

$$\mathcal{L} = -\sum_{\ell} \left[ b_\ell \log p_\ell + (1 - b_\ell) \log(1 - p_\ell) \right]. \tag{8}$$

To minimize the loss function $\mathcal{L}$ with respect to the parameters $W$, the gradient $\nabla_W \mathcal{L}$ must be computed. This gradient is a vector containing the partial derivatives of the loss with respect to each parameter in $W$, indicating the direction in which to adjust the weights to most effectively minimize the loss.

Given the temporal nature of the LSTM processing sequential data, the standard backpropagation algorithm is extended to Backpropagation through time (BPTT). BPTT is used to calculate the gradient $\nabla_W \mathcal{L}$ by unfolding the network over time and applying the chain rule recursively through each time step. This enables the model to learn long-range dependencies within the sequence by propagating the error signal backward through time.

The parameters are subsequently updated using the Adam optimizer. The adaptive learning rate of Adam is particularly suited for the time-varying molecular channel. This joint optimization, driven by BPTT and Adam, enables the equalizer coefficients to converge in a detection-oriented manner, circumventing the need for explicit channel modeling. The overall procedure is shown in Fig. 3, with FNN and LSTM configurations summarized in Table II after data preprocessing.

### B. Numerical Simulation Results

Figures 3 and 4 show the performance of various equalizers at different symbol rates. When $T_b = 4 \cdot t_p$, model-based FDEs generally achieve lower BER with longer symbol lengths. ZF-FDE performs the worst due to noise amplification, while MMSE-FDE outperforms statistical MMSE-FDE at the cost of higher complexity.

Data-driven FDEs consistently surpass model-based approaches. LSTM-FDE achieves the lowest BER, benefiting from its gating mechanism for effective information flow control. GRU-FDE offers intermediate performance, capturing more temporal dependencies than FNN but less long-term modeling capability than LSTM. FNN-FDE exhibits slightly worse performance, with limited gains as the sequence length increases, due to its lack of recurrent structure and constrained temporal feature extraction.

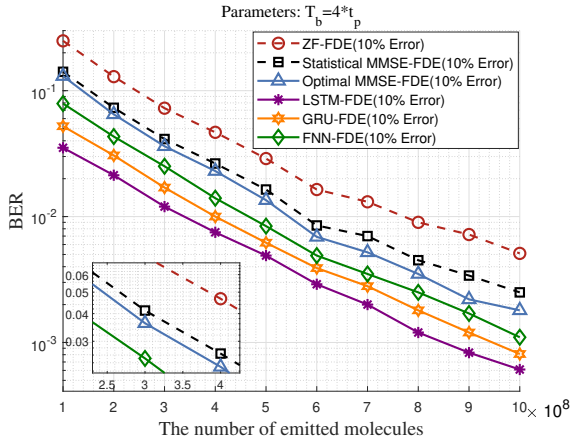


Fig. 5. BER performance comparison under channel estimation errors.

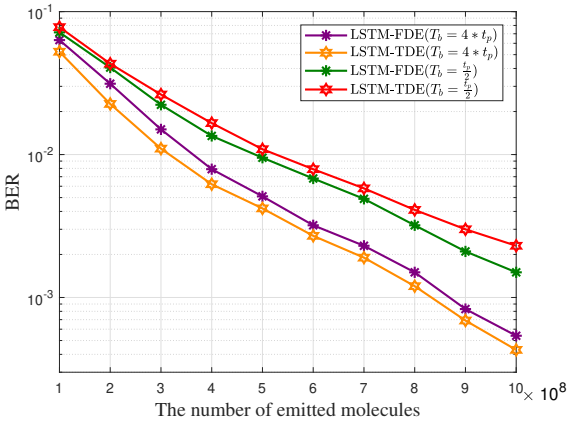


Fig. 6. The BER performance of LSTM-based TDE and FDE at different symbol durations.

Figure 4 compares BER performance at $T_b = t_p/2$, where high symbol rate leads to severe ISI. ZF-FDE performs worst among model-based methods, while optimal and statistical MMSE-FDE exhibit similar BER due to strong noise and ISI. Data-driven FDEs are more robust, with LSTM-FDE achieving the highest gain by leveraging temporal dependencies. GRU- and FNN-FDE perform worse, reflecting a trade-off between complexity and accuracy.

Accurate CIR estimation is essential for optimal equalizer performance. As shown in Fig. 5, when a CIR amplitude perturbation of $\pm 10\%$ occurs, the BER decreases for all schemes as the number of transmitted molecules increases, but the rate of improvement varies. Model-based ZF-FDE and MMSE-FDE, which are highly sensitive to estimation errors, exhibit slower BER reduction under mismatch. In contrast, data-driven approaches show greater robustness, with LSTM-FDE achieving the fastest BER decline due to its strong temporal-dependency modeling and noise suppression, followed by GRU-FDE. FNN-FDE offers limited gain owing to the lack of memory mechanisms. These results highlight that, under channel mismatch, LSTM-FDE can exploit increased molecule counts more effectively to enhance reliability.

Figure 6 compares the performance of LSTM-FDE and LSTM-TDE at varying symbol rates. In low-rate transmissions, both methods exhibit a gradual BER reduction, although the gains taper once the molecule count exceeds a threshold. LSTM-TDE performs slightly better than LSTM-FDE in this regime, but the margin is small. At high symbol rates, LSTM-FDE's block-processing strategy yields a clear advantage, delivering substantially lower BER than LSTM-TDE.

## V. Conclusion

In this letter, we proposed LSTM-FDE, a data-driven frequency-domain equalization scheme for MC systems based on LSTM. By leveraging LSTM's ability to model temporal dependencies, the method achieves high detection accuracy without explicit channel modeling or estimation, learning directly from data. Simulation results show that LSTM-FDE outperforms both model-based FDE and other data-driven baselines across various symbol rates and under channel estimation errors. Compared with its time-domain counterpart, it provides a better trade-off between performance and complexity, making it suitable for high-rate MC scenarios. The approach also exhibits strong robustness in dynamic and noisy channels, highlighting its potential for practical biomedical applications such as in-body monitoring. Future work will explore lightweight recurrent architectures, MIMO extensions, and experimental validation on physical MC platforms.

## References

[1] N. Farsad, H. B. Yilmaz, A. Eckford, C.-B. Chae, and W. Guo, "A comprehensive survey of recent advancements in molecular communication," *IEEE Commun. Surveys Tuts.*, vol. 18, no. 3, pp. 1887–1919, Feb. 2016.

[2] I. F. Akyildiz, M. Pierobon, S. Balasubramaniam, and Y. Koucheryavy, "The Internet of bio-nano things," *IEEE Commun. Mag.*, vol. 53, no. 3, pp. 32–40, Mar. 2015.

[3] C. Lee, B.-H. Koo, C.-B. Chae, and R. Schober, "The Internet of bio-nano things in blood vessels: System design and prototypes," *IEEE/KICS J. Commun. Networks*, vol. 25, no. 2, pp. 222–231, April 2023.

[4] M. Pierobon and I. F. Akyildiz, "Diffusion-based noise analysis for molecular communication in nanonetworks," *IEEE Trans. Signal Process.*, vol. 59, no. 6, pp. 2532–2547, Jun. 2011.

[5] V. Jamali, A. Ahmadzadeh, W. Wicke, A. Noel, and R. Schober, "Channel modeling for diffusive molecular communication—a tutorial review," *Proc. IEEE.*, vol. 107, no. 7, pp. 1256–1301, Jul. 2019.

[6] N. Farsad, "Molecular communication: Interconnecting tiny nanobio devices," *GetMobile-MOBCOMPU.*, vol. 22, no. 2, pp. 5–10, Sep. 2018.

[7] D. Kilinc and O. B. Akan, "Receiver design for molecular communication," *IEEE J. Sel. Areas Commun.*, vol. 31, no. 12, pp. 705–714, Dec. 2013.

[8] N.-R. Kim and C.-B. Chae, "Molecular MIMO: From theory to prototype," *IEEE J. Sel. Areas Commun.*, vol. 34, no. 3, pp. 600–614, Mar. 2016.

[9] G. Yaylali, B. C. Akdeniz, T. Tugcu, and A. E. Pusane, "Channel modeling for multi-receiver molecular communication systems," *IEEE Trans. Commun.*, vol. 71, no. 8, pp. 4499–4512, Aug. 2023.

[10] Y. Huang, F. Ji, Z. Wei, M. Wen, X. Chen, Y. Tang, and W. Guo, "Frequency domain analysis and equalization for molecular communication," *IEEE Trans. Signal Process.*, vol. 69, pp. 1952–1967, Mar. 2021.

[11] K. Xu, M. Qin, F. Sun, Y. Wang, Y.-K. Chen, and F. Ren, "Learning in the frequency domain," in *Proc. IEEE/CVF Conf. Comput. Vis. Pattern Recognit. (CVPR)*, June 2020, pp. 1740–1749.

[12] H. B. Yilmaz, A. C. Heren, T. Tugcu, and C.-B. Chae, "Three-dimensional channel characteristics for molecular communications with an absorbing receiver," *IEEE Commun. Lett.*, vol. 18, no. 6, pp. 929–932, Jun. 2014.

[13] C. Xiang *et al.*, "Hybrid recurrent neural network for signal-dependent noise suppression in molecular communication," *IEEE Trans. Mol. Biol. Multi-Scale Commun.*, vol. 11, no. 2, pp. 283–291, Feb. 2025.